Acta Cryst. (1966). **20**, 264

The Crystal Structures of $NbTe_2$ and $TaTe_2$

BY BRUCE E. BROWN*

Research Division 3325, *Allis-Chalmers Manufacturing Company, Milwaukee* 1, *Wisconsin, U.S.A.*

(*Received* 2 *November* 1964 *and in revised form* 30 *June* 1965)

The crystal structures of the isostructural compounds, $NbTe_2$ and $TaTe_2$, have been solved by Patterson methods. Single crystals were grown by vapor transport methods. Cell dimensions, as measured on precession photographs, are for $NbTe_2$, $a=19{\cdot}39$, $b=3{\cdot}642$, $c=9{\cdot}375$ Å, $\beta=134°35'$, and for $TaTe_2$, $a=19{\cdot}31$, $b=3{\cdot}651$, $c=9{\cdot}377$ Å, $\beta=134°13'$. Both compounds belong to the space group $C2/m$.

Refinement of the $h0l$ intensities by least-squares methods gave R values of 13% and 10% for $NbTe_2$ and $TaTe_2$ respectively. The compounds are layer structures with distorted octahedral coordination of the metal atoms by tellurium atoms. The distortion is a response to a pattern of metal–metal bonding in which the metals are grouped into triple rows parallel to the y axis. This grouping puts two-thirds of the metal atoms in distorted octahedra and one-third in relatively regular octahedra.

Introduction and experimental

During the course of study of possible thermoelectric materials, crystals of the ditellurides of niobium and tantalum were prepared by vapor transport methods (Nitsche, Bolsterli & Lichtensteiger, 1961). The crystals were grown using an iodine carrier for the niobium or tantalum and a gradient of 925 to 650°C between the hot and cold ends of the evacuated quartz tube. The crystals grow in elongated plates or laths whose long dimension is parellel to the short b axis and whose short dimension is perpendicular to the layering of the structure. The cell dimensions, as measured from precession photographs with Mo $K\alpha$ radiation, are for $NbTe_2$: $a=19{\cdot}39$, $b=3{\cdot}642$, $c=9{\cdot}375$ Å, and $\beta=134°35'$, and for $TaTe_2$: $a=19{\cdot}31$, $b=3{\cdot}651$, $c=9{\cdot}377$ Å, and $\beta=134°13'$. The systematic absence of reflections with $h+k=2n+1$ indicated a C-centered monoclinic cell with the possible space groups $C2/m$, Cm, or $C2$.

A summary of the crystallographic data on the tellurides of tantalum and niobium, as reported by other workers, is given in Table 1. Powder data published by these workers match closely our powder data and show our material and theirs to be essentially identical. Table 1 contains the approximate relations between the monoclinic lattice parameters determined from our precession photographs (subscripted m) and other published parameters. The pseudotrigonal symmetry of the lattice, apparent on precession photographs, is apparently responsible for the choice of hexagonal and orthohexagonal cells.

Chemical analyses from the vapor-transported batches of the two compounds give the formulas $Nb_{1{\cdot}02}Te_2$ and $Ta_{0{\cdot}94}Te_2$ if two tellurium atoms per formula unit are assumed. Additional studies made in this laboratory (Revolinsky, Brown, Beerntsen & Armitage, 1965) indicate a small homogeneity range for $NbTe_2$ but $TaTe_2$ is homogenous up to a composition of TaTe.

Densities measured by pycnometric methods are lower than theoretical densities, and lower than densities for these compounds measured by Brixner (1962) and Chaigneau & Santarromana (1963). The tabulated values are, in g.cm^{-3}:

	Brown	Brixner	Chaigneau	Theoretical
$NbTe_2$	6·8	7·6	7·4	7·37
$TaTe_2$	8·4	9·4	–	9·16

Our density measurements, if correct, correspond to about 5·6 formula units per cell rather than the ideal 6 units. The low density values are not understood, although density measurement on these thin crystals is difficult and subject to error. The structures were solved and refined with the assumption of six formula units per cell.

Peak intensity measurements were made on $h0l$ Weissenberg photographs using a standard visual scale. These were first corrected for absorption using the

Table 1. *Published parameters for* $NbTe_2$ *and* $TaTe_2$ *derived from powder photographs, and their approximate relations to the monoclinic cell parameters measured from* $NbTe_2$ *and* $TaTe_2$ *single crystals*

Ukrainskii, Kovba, Simanov & Novoselova (1959) Orthorhombic (pseudohexagonal) $TaTe_{1{\cdot}5}$–$TaTe_2$	Brixner (1962) Rhombohedral (hexagonal axes) $TaTe_2$	Brixner (1962) Rhombohedral (hexagonal axes) $NbTe_2$	Chaigneau & Santarromana (1963) Hexagonal $NbTe_2$
$a=6{\cdot}41$ kX $=\frac{1}{2}a_m$			
$b=10{\cdot}9$ kX $=3b_m$	$a=10{\cdot}9$ Å,	$10{\cdot}9$ Å $=3b_m$	$a=10{\cdot}6$ Å $=3b_m$
$c=6{\cdot}64$ kX $=c_m \sin\beta$	$c=20{\cdot}08$ Å,	$19{\cdot}88$ Å $=3c_m \sin\beta$	$c=20{\cdot}0$ Å $=3c_m \sin\beta$

---

* Present address: Geology Department, University of Wisconsin-Milwaukee, Milwaukee, Wisconsin, U.S.A.

program ORABS of Wehe, Busing & Levy (1962). Both the $NbTe_2$ and $TaTe_2$ crystals were thin laths with dimensions $0{\cdot}005 \times 0{\cdot}2 \times 1$ mm. The longest (1 mm) dimension was parallel to the rotation axis and so had no effect on the zero-level absorption calculations. Following the absorption corrections the intensities were corrected for Lorentz and polarization effects. A scale factor, $[0{\cdot}378\,(\sin\theta/\lambda)^2+1{\cdot}0]$, was applied to each F_o, up to $(\sin\theta/\lambda)^2=0{\cdot}6$ in order to allow for the effect of α_1–α_2 splitting. Beyond $(\sin\theta/\lambda)^2=0{\cdot}6$ splitting is judged complete for Mo $K\alpha$ radiation and the factor was assumed constant at $(1{\cdot}5)^{\frac{1}{2}}=1{\cdot}226$.

Solution of the structure

The short b axis was used as the rotation axis for the Weissenberg zero- and upper-level photographs. Inspection of these showed that all levels with k even had sensibly identical intensities and all levels with k odd were likewise similar. This indicates that all atoms are located on planes with y equal to either 0 or $\frac{1}{2}$. The Patterson projection $P(u, w)$ showed an arrangement of peaks suggesting a distorted octahedral coordination of the metal atoms. Several types of distortion were tried without success. About this time, work on the WTe_2 structure was completed, this also being a layer structure with distorted octahedral coordination of metal atoms. Similarities between the $NbTe_2$ and WTe_2 compounds encouraged us to look for short metal–metal distances between the distorted octahedra. A minimum function solution using these supposed metal–metal vectors gave a consistent trial model. This model is centric with space group $C2/m$.

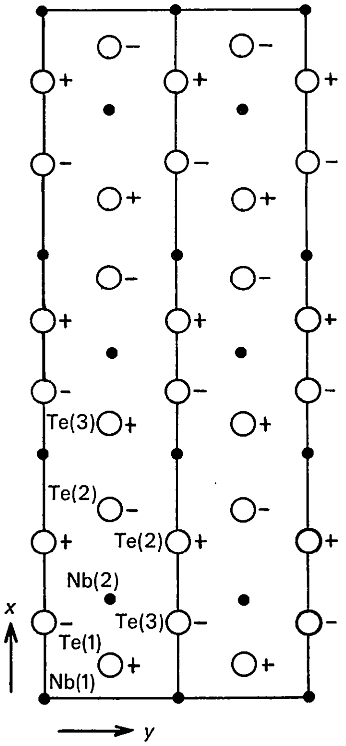

Fig. 1. Projection of a single tellurium–metal–tellurium layer onto the (001) face in a direction perpendicular to (001). Open circles: tellurium; closed circles: niobium or tantalum. Tellurium atoms marked with a plus and minus are above and below the metal atom sheet respectively.

Refinements of both structures were carried out with the full-matrix least-squares program of Busing & Levy (1959). The scattering factors of Thomas & Umeda (1957) were used in the refinement of both compounds. The reflections were weighted according to the relation $w^{\frac{1}{2}}=1{\cdot}0/0{\cdot}1(|F_o|)$. Very weak reflections were given reduced weight and unobserved reflections were given zero weight. For $NbTe_2$ the maximum parameter shift on the final cycle was $0{\cdot}07\sigma$. The average positional parameter shift was $0{\cdot}04\sigma$ and the average temperature factor shift was $0{\cdot}03\sigma$. The final R value is 12·7% and the weighted R is 15·8%. For $TaTe_2$ the maximum parameter shift on the final cycle was $0{\cdot}008\sigma$, the average positional parameter shift $0{\cdot}004\sigma$, and the average temperature factor shift $0{\cdot}004\sigma$. The final R value is 10·4% and the weighted R value is 12·2%.

Description of the structures

The nature of the distortion of the coordinating octahedra in these layer structures is illustrated in Figs. 1

Table 2. *Final parameters for* $NbTe_2$ *and* $TaTe_2$

Atom	$x(\sigma x)$	y	$z(\sigma z)$	$B(\sigma_B)$
		$NbTe_2$		
Nb(1)	0	0	0	0·68(11)
Nb(2)	0·1397(4)	$\frac{1}{2}$	−0·0118(8)	0·72(8)
Te(1)	0·1497(3)	$\frac{1}{2}$	0·2898(6)	0·61(5)
Te(2)	0·2970(3)	0	0·2148(6)	0·63(6)
Te(3)	0·4961(3)	$\frac{1}{2}$	0·3020(6)	0·60(5)
		$TaTe_2$		
Ta(1)	0	0	0	0·30(9)
Ta(2)	0·1396(3)	$\frac{1}{2}$	−0·0111(6)	0·32(6)
Te(1)	0·1483(5)	$\frac{1}{2}$	0·2851(10)	0·79(11)
Te(2)	0·2972(4)	0	0·2179(9)	0·59(11)
Te(3)	0·4944(4)	$\frac{1}{2}$	0·2975(10)	0·84(11)

Table 3. *Bond distances for* $NbTe_2$ *and* $TaTe_2$ (Å)

$NbTe_2$			$TaTe_2$		
Atom 1–atom 2		$d(\sigma_a)$	Atom 1–atom 2		$d(\sigma_a)$
Nb(1)	Nb(2)(4)	3·329(5)	Ta(1)	Ta(2)(4)	3·317(4)
Nb(2)	Nb(2)	4·510(10)	Ta(2)	Ta(2)	4·507(8)
(M–X distances in centric octahedron)					
Nb(1)	Te(1)(4)	2·836(4)	Ta(1)	Te(1)(4)	2·828(6)
Nb(1)	Te(3)(2)	2·880(5)	Ta(1)	Te(3)(5)	2·866(7)
(M–X distances in acentric octahedron)					
Nb(2)	Te(1)(1)	2·690(7)	Ta(2)	Te(1)(1)	2·663(8)
Nb(2)	Te(2)(2)	2·835(6)	Ta(2)	Te(2)(2)	2·845(6)
Nb(2)	Te(2)(1)	2·908(7)	Ta(2)	Te(2)(1)	2·923(7)
Nb(2)	Te(3)(2)	2·754(6)	Ta(2)	Te(3)(2)	2·747(7)
(X–X distances parallel to layering)					
Te(1)	Te(2)	3·837(6)	Te(1)	Te(2)	3·811(8)
Te(2)	Te(3)	3·808(6)	Te(2)	Te(3)	3·798(8)
Te(1)	Te(3)	3·560(5)	Te(1)	Te(3)	3·558(7)
(X–X distances between layers)					
Te(1)	Te(1)	3·527(8)	Te(1)	Te(1)	3·595(12)
Te(1)	Te(2)	3·967(7)	Te(1)	Te(2)	3·999(10)
Te(2)	Te(3)	3·788(7)	Te(2)	Te(3)	3·798(8)
Te(3)	Te(3)	3·600(9)	Te(3)	Te(3)	3·651(14)

Table 4. *Bond angles for* $NbTe_2$ *and* $TaTe_2$ (°)

$NbTe_2$	Angle (σ)	$TaTe_2$	Angle (σ)
Nb(2)–Nb(1)–Nb(2)	66·3(1)	Ta(2)–Ta(1)–Ta(2)	66·8(1)
	(Angles in centric octahedron)		
Te(1)–Nb(1)–Te(1)	79·9(2)	Te(1)–Ta(1)–Te(1)	80·4(2)
Te(1)–Nb(1)–Te(3)	77·0(1)	Te(1)–Ta(1)–Te(3)	77·3(2)
Te(1)–Nb(1)–Te(1)	100·1(2)	Te(1)–Ta(1)–Te(1)	99·6(2)
Te(1)–Nb(1)–Te(3)	103·0(1)	Te(1)–Ta(1)–Te(3)	102·7(2)
	(Angles in acentric octahedron)		
Te(2)–Nb(2)–Te(2)	79·9(2)	Te(2)–Ta(2)–Te(2)	79·8(2)
Te(1)–Nb(2)–Te(2)	87·9(2)	Te(1)–Ta(2)–Te(2)	87·5(2)
Te(1)–Nb(2)–Te(3)	110·5(2)	Te(1)–Ta(2)–Te(3)	110·5(2)
Te(2)–Nb(2)–Te(2)	76·5(2)	Te(2)–Ta(2)–Te(2)	77·2(2)
Te(2)–Nb(2)–Te(3)	95·5(1)	Te(2)–Ta(2)–Te(3)	95·4(2)
Te(2)–Nb(2)–Te(3)	84·5(2)	Te(2)–Ta(2)–Te(3)	84·0(2)
	(X–X–X angles)		
Te(1)–Te(2)–Te(3)	120·5(1)	Te(1)–Te(2)–Te(3)	120·4(2)
Te(3)–Te(1)–Te(2)	120·5(1)	Te(3)–Te(1)–Te(2)	120·2(1)
Te(2)–Te(3)–Te(1)	119·7(1)	Te(2)–Te(3)–Te(1)	119·5(1)
Te(2)–Te(2)–Te(2)	61·6(2)	Te(2)–Te(2)–Te(2)	60·9(2)

Table 5. F_o *and* F_c *values for* $NbTe_2$ *and* $TaTe_2$

ℓ	Fo	Fc
$NbTe_2$		
00ℓ		
2	151	-126
3	185	160
4	222	176
5	0	0
6	64	56
7	101	80
8	25	-18
9	37	30
10	139	95
11	0	1
12	55	-38
13	50	39
14	52	43
20ℓ		
1	54	-40
2	89	100
3	130	124
4	72	-77
5	69	-52
6	151	125
7	84	70
8	66	-49
9	0	9
10	80	55
11	0	7
12	0	11
13	40	30
40ℓ		
0	24	20
1	60	-51
2	107	-108
3	0	-3
4	61	54
5	28	-25
6	77	-67
7	0	-19
8	0	18
60ℓ		
0	203	221
1	126	139
2	64	-62
3	30	32
4	77	64
5	19	-18
6	35	34
7	75	61
8	40	-35
9	35	-30
10	63	51
11	0	22
80ℓ		
0	109	107
1	58	-62
2	32	34
3	190	181
4	43	40
5	71	-58
6	71	57
7	110	82
8	0	1
9	0	12
10	40	35
10.0ℓ		
0	46	44
1	17	19
2	41	-49
3	27	-36
4	0	14
5	37	30
6	0	5
7	0	-25
8	0	-11
9	37	26
12.0ℓ		
0	23	19
1	42	49
2	29	-30
3	0	10
4	0	16
5	62	-51
6	0	-11
7	49	46
8	0	-8
9	40	-42
14.0ℓ		
0	145	160
1	13	-16
2	37	-46
3	86	98
4	83	73
5	31	-24
6	0	10
7	45	39
16.0ℓ		
0	28	24
1	35	41
2	29	31
3	0	7
4	0	-11
5	0	16
6	48	45
18.0ℓ		
0	27	-12
1	0	-4
2	38	-37
3	0	6
4	0	26
5	34	-29
$\bar{2}0\ell$		
3	98	82
4	69	56
5	104	-93
6	64	-49
7	78	67
8	27	26
9	58	-48
10	34	-30
11	0	7
12	0	11
13	0	-2
14	21	-18
$\bar{4}0\ell$		
3	44	-41
4	121	-112
5	14	13
6	125	107
8	115	-99
9	48	38
10	80	60
11	36	-28
$\bar{6}0\ell$		
1	122	-112
2	76	-71
3	248	299
4	160	150
5	112	-89
6	78	69
7	145	127
8	0	8
9	62	56
10	98	88
11	0	-19
12	0	-1
13	120	91
14	45	34
15	45	-34
$\bar{8}0\ell$		
1	121	135
2	30	32
3	85	92
4	61	63
5	44	-39
6	83	74
7	143	140
8	19	-14
9	64	-59
10	62	52
11	77	62
$\overline{10}.0\ell$		
1	26	-34
2	67	-72
3	34	-37
4	0	-3
5	30	29
6	11	-11
7	110	-104
8	51	-45
9	75	69
10	0	5
11	95	-82
$\overline{12}.0\ell$		
1	115	-122
2	27	28
3	174	193
4	45	-50
5	122	-146
6	113	116
7	133	119
8	62	-53
9	12	13
10	68	64
11	0	-18
12	0	25
13	91	82
14	0	-12
15	46	-35
16	72	56
17	63	46
$\overline{14}.0\ell$		
1	76	90
2	32	-32
3	61	73
4	92	103
5	25	29
6	103	109
7	113	109
8	37	-34
7	55	-41
9	22	21
10	164	145
11	63	52
12	39	-40
13	37	27
14	47	63
$\overline{16}.0\ell$		
1	0	-20
2	8	-9
3	51	55
4	52	51
5	10	-14
6	36	-38
7	11	-4
8	46	46
9	39	36
10	50	-46
11	63	-52
12	33	31
13	34	34
$\overline{18}.0\ell$		
1	39	-47
2	29	34
3	29	36
4	110	-119
5	56	-62
6	105	122
7	0	8
8	136	-130
9	0	5
10	64	61
11	43	-35
12	0	-5
13	34	31
14	0	-39
15	0	-13
16	39	61
$\overline{20}.0\ell$		
0	89	104
1	0	-20
2	58	-60
3	70	87
4	76	82
5	0	-16
6	41	45
7	57	61
8	0	-13
9	60	66
10	119	118
11	0	-15
12	27	-30
13	103	94
14	86	73
$\overline{22}.0\ell$		
0	0	16
1	18	23
2	36	37
3	65	63
4	30	30
5	0	-14
6	28	31
7	73	83
8	42	44
9	0	-9
10	0	-2
11	42	40
12	61	56
13	0	10
14	18	-26
$\overline{24}.0\ell$		
0	0	14
1	0	-10
2	0	5
3	0	-10
4	45	-51
5	0	18
6	53	60
7	60	-64
8	70	-86
9	50	55
10	38	38
11	72	-72
12	31	-25
13	12	21
14	29	-28
15	0	-6
16	29	26
$\overline{26}.0\ell$		
0	0	26
1	44	-60
2	14	-22
3	64	77
4	0	5
5	61	-68
6	0	22
7	39	44
8	16	-22
9	16	24
10	35	39
11	43	-44
12	0	4
13	95	92
14	0	7
15	52	-52
16	41	34
17	52	57
$\overline{28}.0\ell$		
0	0	28
1	0	32
2	0	15
3	20	25
4	0	16
5	0	9
6	54	56
7	62	62
8	0	-2
9	0	0
10	60	63
11	61	63
12	0	15
13	0	2
14	23	23
16	38	35
$\overline{30}.0\ell$		
0	0	16
1	0	-6
2	0	3
3	0	13
4	0	8
5	20	25
6	0	11
7	34	-36
8	0	2
9	65	66
10	0	-2
11	54	-61
12	0	15
13	44	41
$\overline{32}.0\ell$		
0	0	-3
1	33	-34
2	0	10
3	30	37
4	37	-40
5	40	-48
6	33	40
7	20	19
8	41	-50
9	0	-4
10	0	15
11	24	-32
12	0	7
13	35	36
14	43	-43
15	41	-37
16	52	53
17	0	21
18	45	-46
$\overline{34}.0\ell$		
10	59	60
14	49	47
$\overline{36}.0\ell$		
8	34	32
9	26	31
10	0	-13
11	0	-7
12	45	49
13	33	31
$TaTe_2$		
00ℓ		
2	54	-44
3	231	234
4	279	267
5	73	73
6	100	97
7	135	138
8	0	54
9	0	69
10	102	123
20ℓ		
2	141	118
3	224	149
4	0	-34
5	0	-26
6	157	148
7	100	110
8	0	-17
9	0	26
10	94	91
40ℓ		
0	11	-8
1	86	-76
2	142	-129
3	0	-28
4	0	30
5	41	-46
6	85	-88
60ℓ		
0	253	273
1	180	201
2	0	-18
3	55	53
4	141	106
5	0	25
6	0	44
7	66	72
80ℓ		
0	197	172
1	0	9
2	88	89
3	231	233
4	0	107
5	0	-6
6	65	95
7	115	139
10.0ℓ		
0	33	29
1	0	7
2	58	-58
3	45	-42
12.0ℓ		
0	0	11
1	63	58
14.0ℓ		
0	208	215
1	60	51
16.0ℓ		
0	48	48
1	61	69
$\bar{2}0\ell$		
3	103	83
4	79	56
5	93	-86
6	46	-51
7	57	60
8	0	23
9	52	-57
$\bar{4}0\ell$		
3	74	-59
4	130	-123
5	0	-4
6	108	91
7	0	-42
8	108	-106
9	0	29
10	54	68
$\bar{6}0\ell$		
1	64	-53
2	0	-4
3	360	366
4	232	225
5	15	-27
6	136	119
7	202	203
8	110	82
9	87	93
10	132	134
11	0	50
12	0	46
13	112	121
14	71	82
$\bar{8}0\ell$		
1	218	194
2	122	98
3	180	149
4	153	121
5	0	22
6	133	117
7	185	174
8	31	26
9	0	-27
10	56	74
11	70	89
$\overline{10}.0\ell$		
1	58	-50
2	116	-89
3	73	-56
4	27	-25
5	0	2
6	43	-36
7	143	-123
8	78	-67
9	0	45
10	0	-11
11	104	-102
$\overline{12}.0\ell$		
1	129	-119
2	37	43
3	202	201
4	38	-36
5	143	-128
6	162	133
7	165	152
8	21	-27
9	33	22
10	98	96
11	0	29
12	0	44
13	100	97
$\overline{14}.0\ell$		
1	160	147
2	52	42
3	168	143
4	185	173
5	126	106
6	170	173
7	180	172
8	38	41
9	86	83
10	189	194
11	107	110
$\overline{16}.0\ell$		
1	0	0
2	0	12
3	75	74
4	65	65
5	0	-2
6	21	-27
7	21	4
8	51	50
9	24	34
10	45	-47
11	49	-54
$\overline{18}.0\ell$		
1	50	-62
2	0	23
3	0	11
4	141	-139
5	81	-74
6	131	102
7	23	-6
8	156	-143
9	0	-12
10	70	59
11	40	-34
$\overline{20}.0\ell$		
0	105	121
1	0	5
2	0	-18
3	121	120
4	127	116
5	0	31
6	111	87
7	119	106
8	51	45
9	129	112
10	184	158
11	0	42
12	0	22
13	121	135
14	125	123
$\overline{22}.0\ell$		
0	0	58
1	0	64
2	83	86
3	110	110
4	70	73
5	0	33
6	84	78
7	133	124
8	83	84
9	0	29
10	0	33
11	85	75
12	84	85
13	0	33
14	0	-5
$\overline{24}.0\ell$		
0	0	6
1	0	-7
2	0	3
3	0	-25
4	58	-58
5	0	12
6	53	43
7	91	-79
8	104	-98
9	30	37
10	0	23
11	95	-88
12	66	-51
$\overline{26}.0\ell$		
0	0	10
1	0	-63
2	0	-16
3	67	70
4	0	2
5	61	-57
6	34	25
7	33	48
8	0	-5
9	32	31
10	57	47
$\overline{28}.0\ell$		
0	0	56
1	0	65
2	0	59
3	0	65
4	0	54
5	64	58
6	99	105
7	96	105
8	35	47
9	35	52
10	111	111

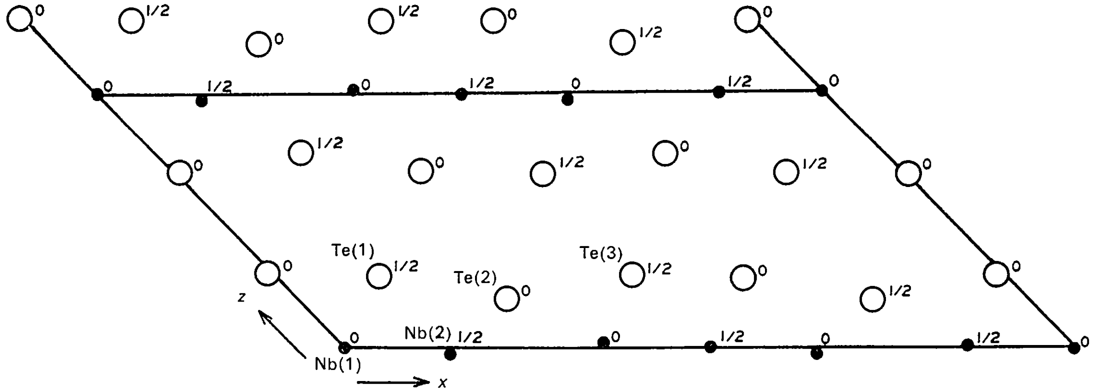

Fig. 2. Projection of the $NbTe_2$ structure onto the (010) face. Open circles: tellurium atoms; closed circles: niobium atoms. The fractional y coordinates are denoted by 0 or $\frac{1}{2}$.

and 2. Fig. 1 is a projection of a single tellurium–metal–tellurium layer onto the (001) face and shows the two environmentally distinct types of metal atom. The rows of metal atoms parallel to y are not spaced at equal intervals along x but have been shifted so that groups of three rows each are formed, that is, two outer rows (containing Nb(2) atoms inside distorted octahedra of Te atoms) have shifted towards a central row (containing Nb(1) atoms within relatively undistorted octahedra). The metal atoms in the central row of relatively undistorted octahedra have four near metal neighbors at approximately 3·3 Å while the metal atoms in the two outside metal rows, in octahedra distorted by their off center position, have two near metal neighbors. Fig. 2, a (010) projection of the structure, illustrates the distortion parallel to z. The rippling of the tellurium sheets is apparently a response to the asymmetric character of the metal–metal distances. Where metal–metal distances are short, tellurium–tellurium distances transverse to the layering are lengthened; where metal–metal distances are long, the transverse tellurium distances are shortened. The tellurium surface thus appears as a series of troughs and crests, the 'wave length' of which is $a/2$. The metal atoms also do not fall exactly into perfect plane layers as can be seen in Fig. 2. The stacking of adjacent layers is keyed by an association of the troughs and crests as is evident from examination of Fig. 2. The preferred growth direction of these crystals is parallel to the troughs and crests of this wave system.

Discussion

As in $MoTe_2$, WTe_2 (Brown, 1966) and numerous other transition metal compounds (Marinder & Magnéli, 1957) exhibiting less than their maximum valence, $TaTe_2$ and $NbTe_2$ have metal–metal bonding. The pattern of metal–metal bond lengths shown by these compounds emphasizes the relation between the number of electrons available for bonding and the bond length, a relation pointed out by Marinder & Magnéli (1957). Thus the metal–metal bond lengths in the molybdenum and tungsten tellurides are shorter with respect to the elemental length than in the tantalum and niobium tellurides.

In the molybdenum and tungsten tellurides the metal–metal bonds occur between atoms on a zigzag chain formed by staggering two parallel rows of metal atoms. Each metal atom forms two metal–metal bonds in this arrangement. The three-row arrangement described above for the niobium and tantalum tellurides allows an average of $2\frac{2}{3}$ metal–metal bonds per atom (two atoms with four such bonds, and four atoms with two). These differences in metal–metal coordination do not result in differences in bond lengths relative to the corresponding dioxides (where metal–metal bonds occur between isolated pairs). Thus the ratios of the distance, metal–metal (telluride)/metal–metal (dioxide), are almost the same for the molybdenum–tungsten compounds as for the niobium–tantalum compounds.

The Nb_3Te_4 and Nb_3Se_4 phases studied by Selte & Kjekshus (1964), although not structurally identical, are similar to the $NbTe_2$ and $TaTe_2$ phases since all these phases exhibit distorted octahedral coordination of metal atoms in response to metal–metal bonding.

References

Brixner, L. H. (1962). *J. Inorg. Nuclear Chem.* **24**, 257.
Brown, B. E. (1966). *Acta Cryst.* **20**, 268.
Busing, W. & Levy, H. A. (1959). Oak Ridge National Laboratory, Central Files No. 59-4-37.
Chaigneau, M. & Santarromana, M. (1963). *C. R. Acad. Sci., Paris,* **256**, 1797.
Marinder, B. & Magnéli, A. (1957). *Acta Chem. Scand.* **11**, 1635.
Nitsche, R., Bolsterli, H. U. & Lichtensteiger, M. (1961). *Phys. Chem. Solids,* **21**, 199.
Revolinsky, E., Brown, B. E., Beerntsen, D. J. & Armitage, C. H. (1965). *J. Less-Common Metals,* **8**, 63.
Selte, K. & Kjekshus, A. (1964). *Acta Cryst.* **17**, 1568.
Thomas, L. H. & Umeda, K. (1957). *J. Chem. Phys.* **26**, 293.
Ukrainskii, Y., Kovba, L. M., Simanov, Y. N. & Novoselova, A. V. (1959). *Zh. Neorg. Khim.* **4**, 2820.
Wehe, D. J., Busing, W. & Levy, H. A. (1962). Oak Ridge National Laboratory, Fortran program ORABS, ORNL-TM-229.